SCIENCE CHINA
Chemistry

• ARTICLES •

October 2011 Vol.54 No.10: 1615–1621
doi: 10.1007/s11426-011-4330-y

Nitrogen-doped carbon nanotube/polyaniline composite: Synthesis, characterization, and its application to the detection of dopamine

FENG XiaoMiao[†*], LI RuiMei[†], MA YanWen, CHEN RunFeng, MEI QunBo, FAN QuLi & HUANG Wei[*]

Key Laboratory for Organic Electronics & Information Displays (KLOEID); Institute of Advanced Materials (IAM), Nanjing University of Posts & Telecommunications (NUPT), Nanjing 210046, China

Received March 18, 2011; accepted May 1, 2011; published online June 27, 2011

Nitrogen-doped carbon nanotubes (N-CNTs)/polyaniline (PANI) composites are developed as an electrode material for biosensors. The morphology, composition, and optical properties of the resulting products were characterized by transmission electron microscopy (TEM), thermogravimetric analysis (TGA), Fourier transform infrared spectroscopy (FT-IR), and ultraviolet-visible absorption spectra (UV-vis). Furthermore, N-CNTs/PANI composite was immobilized on the surface of a glassy carbon electrode (GCE) and applied to construct a sensor. The obtained N-CNTs/PANI-modified GCE showed one pair of redox peaks and high catalytic activity for the oxidation of dopamine (DA) in a neutral environment. Differential pulse voltammograms results illustrate that the fabricated DA biosensor has high anti-interference ability towards ascorbic acid (AA). In addition, the fabricated biosensor showed superior performances with two wide linear ranges from 1 to 80 μM and from 1.5 to 3.5 mM and a low detection limit of 0.01 μM.

nitrogen-doped carbon nanotubes (N-CNTs), polyaniline, biosensors, dopamine

1 Introduction

Carbon nanotube (CNT) has attracted much interest due to its outstanding properties such as electronics, mechanics, and structural characteristics. It has been used to facilitate the immobilization of biological molecules and can serve as a biosensor [1]. For example, it can accelerate electron transfer for a large number of electroactive species and show electrocatalytic activity towards biological compounds such as nicotinamide adenine dinucleotide (NADH) [2], dopamine (DA) [3], and H_2O_2 [4]. Recently, it has been reported that CNT doped with other non-carbon chemical elements (such as boron, nitrogen, etc.) can further improve the mechanics and electrical properties of CNT. The curvature changes the chemically inert graphite surface and makes it easier to incorporate atoms on the tube surface [5]. Among all the potential dopants, nitrogen is considered to be an excellent element for the chemical doping of carbon materials because of its comparable atomic size and five valence electrons available to form strong valence bonds with carbon atoms [6]. The doping of nitrogen to some extent undermines the ordered structure of CNT and creates a certain number of defect sites on the wall. The defects based on the bamboo-shaped N-CNTs can be modified easier than that of pure CNT, resulting in higher functionality and electrochemical activity of N-CNTs. Conjugation of one-pair electrons of nitrogen and the graphene π-system [7] may create nanomaterials with better electronic and mechanical properties [8]. In previous studies, the doping of nitrogen has been successfully employed to modify CNT. For instance, N-dopant increases the metallic behavior, affects the lattice alignment, and regulates the growth mechanism of CNT. Moreover, it has been demonstrated that the doping of nitrogen enhances the biocompatibility and sensitivity of CNTs in biosensing field [9].

†These authors contributed equally to this work.
*Corresponding authors (email: iamxmfeng@njupt.edu.cn; wei-huang@njupt.edu.cn)

Polyaniline (PANI) is one of the most important conducting polymers and has been researched intensively over the past few years due to its ease of synthesis, well electronic and optical properties [10] and environmental stability [11]. Although PANI has many advantages and holds high position among the conducting polymers owing to its unique tunable conductivity either by protonic acid doping or redox doping, its electroactivity can only be retained in acidic media, normally at pH < 4.0 [7]. Such a limitation greatly hinders its application in biological fields. To date, much effort has been made to improve the electrochemical activity of PANI in the neutral condition, which is mainly based on a protonic acid and functional polymer doping mechanism. For example, electroactive PANI in the neutral media has been synthesized either by introducing sulfonic [12], boronic [9], phosphonic [8], carboxyl [13], or acidic groups on the phenyl ring [14] or by doping the PANI with functional polymers, such as poly(vinyl alcohol), poly (ethylene oxide), and poly[(N-vinyl pyrrolidone)-co-(vinyl alcohol)] by copolymerization of aniline with the polyelectrolyte or polyelectrolytemonomer [15].

The fabrication of CNT/PANI composites has attracted great interest in recent years because the incorporation of PANI into CNT can result in new composite materials with enhanced electronic properties. The effective site-selective interaction between the π-bonds in the aromatic rings of the PANI and the graphitic structure of multiwall carbon nanotubes (MWNTs) will strongly facilitate the charge-transfer reaction between the two components. Li *et al*. [16] adopted MWNTs with minimal defects as templates and facilely fabricated CNT/PANI nanocomposites with uniform core-shell structures by ultrasonic assisted *in situ* polymerization. As a result, great improvements in the electrical and electrochemical properties of the resulting nanocomposites were observed. Guo *et al*. [17] produced SWNT-PANI-Au nanoparticles composite in an one-pot fashion. However, the electrochemical activity of SWNT-PANI-Au was not good in neutral conditions. Recently, Komathi *et al*. [18] fabricated a biosensor on the utility of interconnected structure of MWNTs, silica network, and PANI chains for immobilization of a redox enzyme (horseradish peroxidase, HRP), and the direct electrochemistry of HRP could be realized due to synergistic contributions from conducting CNT, electron mediating PANI chains and porous silica network. Although these CNT/PANI composites have been reported, the synthesis and application in biosensing of N-CNTs/PANI nanocomposite with improved electrochemical activity are rarely reported.

In this work, we use simple self-assembly method to fabricate N-CNTs/PANI nanocomposites and then develop a biosensor to the detection of dopamine (DA). The prepared nanocomposites were characterized by means of TEM, TGA, FT-IR, and UV-vis. The TEM results showed that it had an encapsulated structure with the outer layer of PANI and the inner layer of N-CNTs. Furthermore, the fabricated N-CNTs/PANI had high electrochemical activity in neutral even alkaline solutions. Based on the excellent redox properties, the nanocomposite was immobilized on an electrode to construct a DA biosensor. The biosensor showed good reproducibility, stability, and selectivity with two linear responses to DA in the ranges from 1 to 80 μM and from 1.5 to 3.5 mM and a low detection limit of 0.01 μM.

2 Experiment

2.1 Materials

Aniline, hydrochloride(HCl), ammonium persulfate ($(NH_4)_2S_2O_8$, APS), phthalic diglycol diacrylate (PDDA) (M_w: 200,000–350,000), polystyrene sulfonic acid sodium (PSS) (M_w: 70,000), were purchased from Shanghai Chemical Reagent Company. Nafion, a 5 wt% solution in a mixture of lower aliphatic alcohols and 20% water, was obtained from Aldrich. Ascorbic acid (AA) and DA chloride were purchased from Sigma Chemicals and used as received. Other chemicals were of analytical reagent grade and without further purification. Phosphate buffer solution (PBS) was prepared from NaH_2PO_4 (0.1 M) and Na_2HPO_4 (0.1 M) and adjusted the pH with 0.1 M H_3PO_4 and NaOH solutions. Freshly prepared AA and DA solutions were used for all experiments.

2.2 Synthesis of N-CNTs/PANI nanocomposites

N-CNTs (5% nitrogen doped), N-CNTs were prepared, purified, shortened and –COO– introduced processes were as follows [19]: first, the catalyst was removed by 6 M NaOH at 110 °C for 6 h, and then by 6 M HCl at 90 °C for 6 h; second, the N-CNTs was acidificated by HNO_3 at 110 °C for 6 h. In each step, the product was filtered and washed with double distilled water until the filtrate became neutral and finally dried.

250 μL of PDDA was dissolved in 10 mL of 0.5 M NaCl aqueous solution, then 10 mL N-CNTs (2.5 mg/mL) was added to the above solution under stirring for 20 min. After that, the mixture was washed with distilled water for several times to prepare PDDA-modified N-CNTs. PDDA-modified N-CNTs were dispersed into 10 mL PSS (1%) of 0.5 M NaCl aqueous solution under stirring for another 20 min and washed as the above method. Then PSS-modified N-CNTs could be obtained. 100 μL aniline was added to 10 mL PSS-modified N-CNTs of 0.1 M HCl aqueous solutions. After stirring for 30 min, APS was added to the above mixture and the reaction was allowed to proceed overnight. The molar ratio of aniline to APS was 1. After that, the mixture was centrifuged and completely washed with distilled water and ethanol for several times. The final product was dried in vacuum at 80 °C for 24 h.

2.3 Preparation of the N-CNTs/PANI-modified GCE

A GCE was polished to a mirror surface before each experiment with 0.05 μm Al_2O_3 slurry, and then ultrasonicated in distilled water successively. N-CNTs/PANI nanocomposites were dispersed in distilled water to form a 3.0 mg/mL solution and ultrasonically treated for 30 min. The pretreated GCE was cast with 5 μL of the suspension of N-CNTs/PANI nanocomposites. The electrode was then coated with 2 μL of 1% Nafion solution and dried in air.

2.4 Characterization

Ultraviolet-visible (UV-vis) spectra were recorded with a Shimadzu UV-3600 and the samples were dispersed in double-distilled water. Fourier transform infrared (FT-IR) spectra of samples in KBr pellets were recorded with a Bruker model VECTOR22 Fourier transform spectrometer. Transmission electron microscopy (TEM) images were obtained with a JEOL JEM-200CX electron microscope. Thermogravimetry analysis (TGA) was determined using a DTG-60 from room temperature to 800 °C with a heating rate of 10 °C/min in nitrogen atmosphere. Electrochemical experiments were performed on a CHI660C electrochemical workstation (Chenhua Co., Shanghai, China) in a three-electrode configuration. A saturated calomel electrode (SCE) and a platinum electrode served as the reference and counter electrode, respectively. The working electrode was an N-CNTs/PANI-modified GCE.

3 Results and discussion

The shapes of N-CNTs and N-CNTs/PANI nanocomposites have been verified by TEM, as shown in Figure 1. From Figure 1(a) we can see that the pure N-CNTs are tangled rope-like tubes with smooth surface, while the N-CNTs/PANI composite has a network nanostructure with very rough surface. The N-CNTs display a well-dispersed one-dimensional structure with the outer diameter about 30 nm. In the TEM images of N-CNTs/PANI, the outer layer is PANI and the inner layer is constructed by N-CNTs, which indicates the formation of apparent encapsulated structures. The rough, amorphous outer PANI layer has an average thickness of about 30–40 nm.

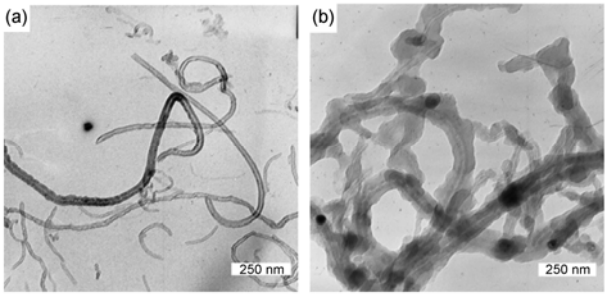

Figure 1 TEM images of N-CNTs (a) and N-CNTs/PANI (b).

Figure 2 presents the TGA curves of N-CNTs, intrinsic PANI, and N-CNTs/PANI composite. The TGA curve of the acid-treated N-CNTs shows a 92% weight loss between 465 and 554 °C, due to the oxidation of carbon into gaseous carbon dioxide. The residual weight percentage refers to the weight percentage content of the iron species present in the N-CNTs structure. The TGA curve of intrinsic PANI (Figure 2(b)) shows a 14% weight loss in the range of 23 and 233 °C, attributing to the loss of water and acid dopants. The large weight loss starting at around 310 °C is believed to the oxidation of the skeletal PANI chain structure [20–22]. The total weight loss of intrinsic PANI is 100% in the experimental conditions. In the case of N-CNTs/PANI composite, TGA curve shows a three-step weight loss. The first weight loss is consistent with the loss of residual water and acid dopants, the next two weight losses in the regions of 309–569°C and 569–584°C are assigned to the oxidation and decomposition of the PANI and N-CNTs, respectively [23]. From the results we can estimate that the percentage content of N-CNTs in the composite is about 12%. The temperature of decomposition for PANI chains in the pure PANI and N-CNTs/PANI is similar because the content of N-CNTs in the composite is low.

Typical UV-vis and FT-IR spectra of N-CNTs, intrinsic PANI, and N-CNTs/PANI are shown in Figure 3. It can be seen that the acid treated N-CNT has a maximum peak at about 250 nm, which is a clear diagnostic of covalent side wall functionalization, i.e. disruption of the conjugated π system [17]. The UV-vis spectrum of PANI exhibits three absorption peaks at 340, 430, and 700 nm, which are the characteristic absorption peaks of the emeraldine oxidation state of PANI. The absorption peaks at 340 and 430 nm are attributed to the π-π* transition of benzenoidrings and polaronic peak reflecting protonation of backbone of the PANI. The peak at 700 nm represents the π-polaron transition indicating that the nanotubes are in the conductive state [24]. The spectrum of N-CNTs/PANI shows that the peaks at 250 nm are consistent with the typical spectra of N-CNTs, but the

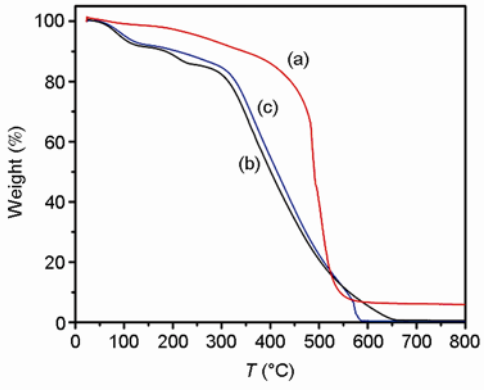

Figure 2 TGA spectra of (a) N-CNTs, (b) PANI, and (c) N-CNTs/PANI.

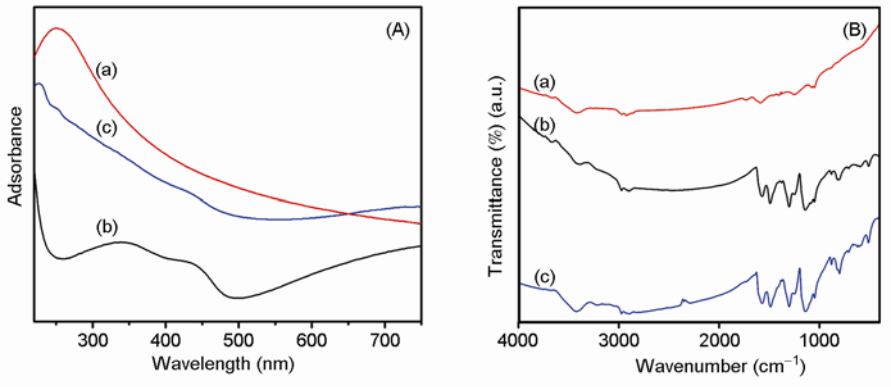

Figure 3 UV-vis (A) and FT-IR (B) spectra of (a) N-CNTs, (b) PANI, and (c) N-CNTs/PANI.

π-π* transition and the π-polaron transition are very weak or lack of observation. It may be covered by the strong absorption peak of N-CNTs in the same region, indicating that PANI can be adsorbed on the N-CNTs surface efficiently. The absorption peak at about 700 nm shows a red shift in the spectrum of N-CNTs/PANI and becomes broader. This result indicates that the interaction between N-CNTs and PANI can increase the effective degree of electron delocalization and facilitate the charge transfer process between the components of the system [25].

In the FT-IR spectrum of N-CNTs (figure 3(2A)), the characteristic vibration modes of the hydroxyl group (~3450 cm^{-1}) and carbonyl group (~1640 cm^{-1}) are observed obviously, demonstrating that N-CNTs have been functionalized with carboxylic and carboxylate groups after treatment with acid [26, 27]. After the assembly of PANI, several new peaks are found in Figure 3B(c). The characteristic peaks at ~1560–1580 cm^{-1} and ~1480–1500 cm^{-1} correspond to the C=C stretching of quinoid and benzenoid rings, those at ~1290–1305 cm^{-1} and ~1235–1245 cm^{-1} are related to the C–N and C=N stretching modes, those at ~1116–1145 cm^{-1} are assigned to the in-plane bending of C–H, and those at ~810–820 cm^{-1} are attributable to the out-of-plane bending of C–H[28]. These characteristic peaks are in agreement with the FT-IR features of pure PANI, indicating that PANI has been effectively assembled on the surface of N-CNTs.

The redox properties of the prepared N-CNTs/PANI composite are characterized by cyclic voltammetric (CV) experiments. Generally, PANI exists in three well-defined oxidation states: leucoemeraldine, emeraldine, and pernigraniline. All of the nitrogen atoms are amines in the leucoemeraldine state and imines in the pernigraniline state, respectively. Emeralding base and emeraldine salt forms can be interchanged depending on the pH value of the solution. For pure PANI, it is only electroactive when the pH is lower than 4.0 [29]. This greatly restricts its applicability in bioelectrochemistry, which normally requires a neutral pH environment. However, when PANI is combined with N-CNTs, the electroactive ability is greatly improved [30]. As shown in Figure 4, the N-CNTs/PANI nanocomposite-modified GCE shows two pairs of redox peaks in solution with pH of 1.0. The first and second oxidation waves correspond to the transition of leucoemeraldine to emeraldine salt and that of emeraldine salt to pernigraniline state in acid media, respectively [31]. With the increasing pH from 5.0 to 8.0, the redox potentials of N-CNTs/PANI modified GCE shifted to more negative values for the reduction process. It still has electroactivity even in PBS with a pH value of 8.0. The redox peaks observed in PBS from pH 5.0 to 8.0 are the overlap of two redox processes for PANI under acidic conditions.

The effect of scan rate (υ) on the peak currents of the N-CNTs/PANI nanocomposite in the range from 50 to 500 mV/s is shown in Figure 5. With the increase of scan rate, the anodic peak potential shifts toward a more positive value and the cathodic peak potential shifts toward a more negative value. Both the anodic and cathodic peak currents for PANI increase linearly with the square root of the scan rate ($\upsilon^{1/2}$), indicating that the peak current is diffusion-controlled.

DA is one of the most important neurotransmitters and it has been implicated in physiological human processes including attention, emotion, motivation and so on [32]. It has

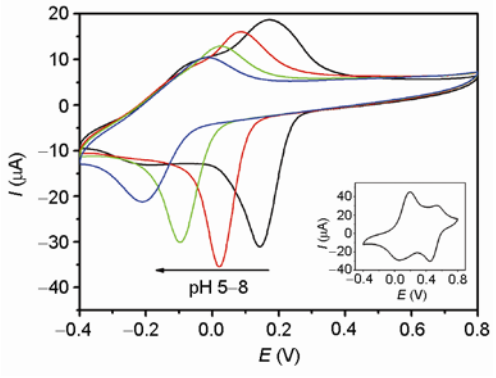

Figure 4 Cyclic voltammograms of N-CNTs/PANI-modified GCE measured in different pH PBS (from 5.0 to 8.0) at a scan rate of 100 mV/s. The inset shows the cyclic voltammogram of N-CNTs/PANI at pH of 1.0.

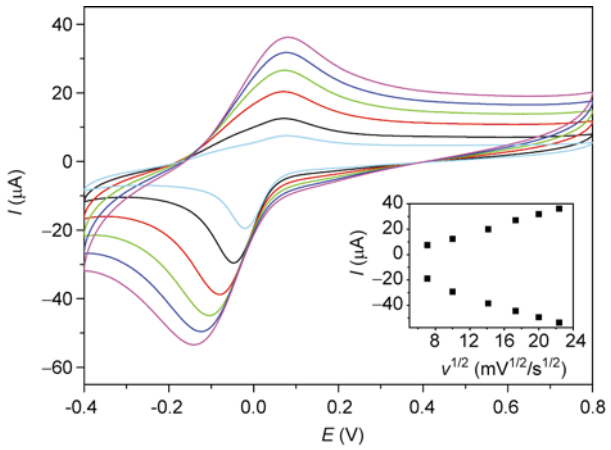

Figure 5 Cyclic voltammograms of N-CNTs/PANI modified GCE in PBS (pH 6.0) at different scan rates: from inside to outside 50, 100, 200, 300, 400, 500 mV/s. Insert shows calibration plots between the cathodic and anodic peak current and the square root of the scan rate.

received much attention in the development of methods for the detection of DA in biological fluids. Electrochemical method has been proven to be rapid, simple, and sensitive. However, there are some problems about electrochemical method due to the oxidative electrode reaction of DA. The main problem of electrochemical detection of DA is the interference from AA, which largely coexists with DA in brain tissue because they have an overlapping oxidation potential [33]. Thus, it is very important to improve the anti-interference ability for the detection of DA.

Based on the excellent electrochemical behaviour of N-CNTs/PANI composite, it was immobilized on the surface of GCE and applied to construct a DA sensor. In the potential range of 0.8 and −0.4 V, CVs of N-CNTs/PANI-modified electrode in different pH PBS (from 5.0 to 8.0) before and after the addition of DA are shown in Figure 6(a) and (b), respectively. A new pair of redox peak occurred after the addition of DA, indicating that the N-CNTs/PANI composite can act as a catalyst for the oxidation of DA. This biosensor shows very good redox activity at neutral pH or even in an alkaline environment in PBS. Besides, the catalytic activity is maximal when pH value is 6.0, indicating that that pH 6.0 is the most suitable.

Simultaneous determination of DA and AA at N-CNTs/PANI-modified GCE was carried out using differential pulse voltammograms (DPV). DPV has much higher sensitivity and better resolution compared to CV. The contribution of charging current to the background current is negligible in DPV [34]. Figure 7 is the DPV obtained at N-CNTs/PANI -modified GCE in pH 6.0 PBS without DA and AA (curve (a)), with 1 mM AA (curve (b)) and 1mM DA (curve (c)), respectively. All curves show an oxidation peak at −0.05 V, corresponding to the transition from leucoemeraldine to pernigraniline.

After the addition of DA, a large oxidation peak of DA appears at 0.19 V, as shown in Figure 7(c). At the same time, the oxidation peak current of N-CNTs/PANI nanocomposites increases due to the interaction between the nanocomposites and DA or its reduction products. However, only a small shoulder peak appears when AA is added (Figure 7(b)). It can be seen that although the concentration of

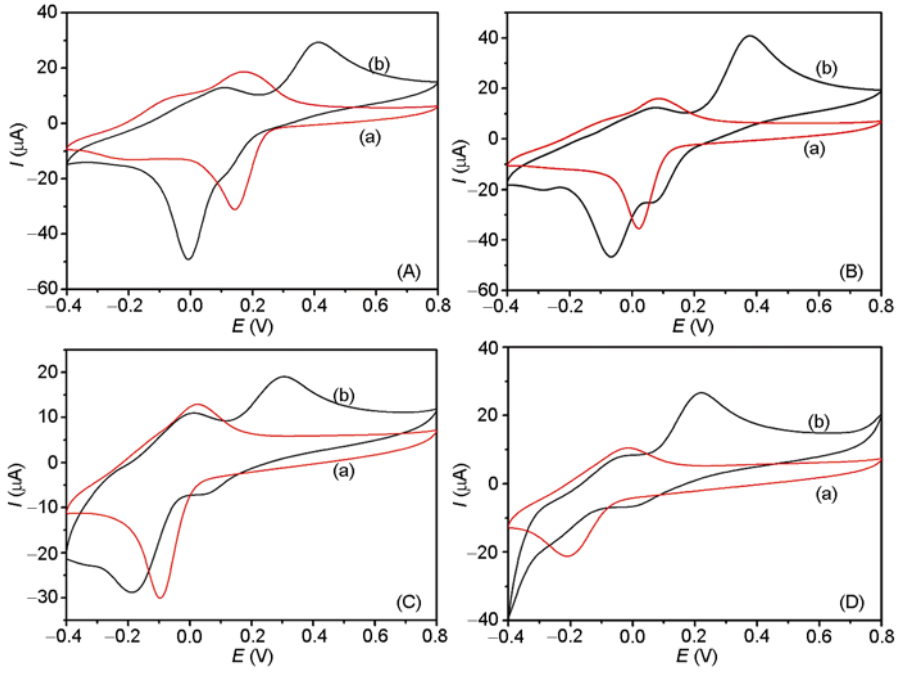

Figure 6 Cyclic voltammograms of N-CNTs/PANI-modified GCE in the absence (a) and presence (b) of DA at different pH of (A) 5.0, (B) 6.0, (C) 7.0, and (D) 8.0 at a scan rate 100 mV/s.

AA and DA is the same, the peak current of DA is much higher than that of AA, indicating DA can be detected in the presence of AA and the anti-interference ability of the biosensor is enhanced. The possible reason is that there may be some interaction between AA and N-CNTs/PANI nanocomposites, which has hampered oxidation of AA [32].

To further investigate the electrocatalytic ability of the N-CNTs/PANI-modified GCE, amperometric detection of DA at constant potential was carried out. Figure 8 shows the current-time curve of the biosensor on successive addition of DA in 0.1 M PBS solution (pH 6.0) at an applied potential of 375 mV. The biosensor showed two linear responses to DA concentration in the ranges from 1 to 80 μM and from 1.5 to 3.5 mM, with a low detection limit of 0.01 μM. The performance of this DA biosensor is much better than the reported data [35]. The high sensitivity in detecting DA suggested that N-CNTs/PANI enhanced efficiency of electron transfer between DA and the electrode greatly.

The effect of possible interfering species on DA detection was examined using the same concentration of AA, uric acid, and glucose, which caused an increase of 8.0%, 7.0%, and 2.0% in the oxidation current of 1mM DA, respectively. This result suggested that the proposed biosensor has high selectivity, and has little interference from the endogenously coexisted electroactive substances.

The reproducibility and stability of the biosensor was investigated by successively detecting 1 mM DA for 6 times, the relative standard deviation (RSD) was 0.5%, demonstrating a good reproducibility. After 100 successive scanning the response still retained 96% value of the initial response, suggesting the acceptable durability of the biosensor. In addition, the RSD of current signals for measurement of 1 mM DA at five independently prepared biosensors was 4.2%, proving the good reproducibility of the biosensor. When N-CNTs/PANI-modified GCE was stored at 4 °C and measured at intervals over several days, no obvious decrease in the response to DA was observed after seven days.

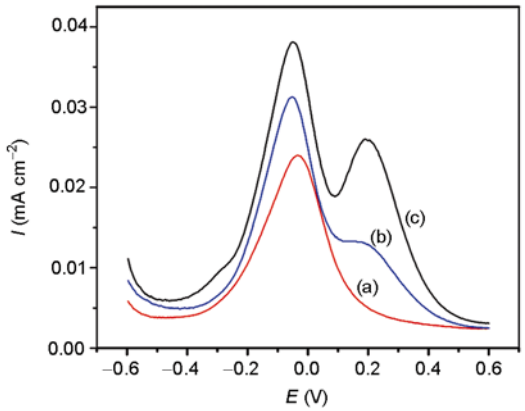

Figure 7 Differential pulse voltammograms of N-CNTs/PANI-modified GCE in 0.1 M pH 6.0 PBS. Blank (a), (a) +1 mM AA (b), and (a) + 1mM DA (c).

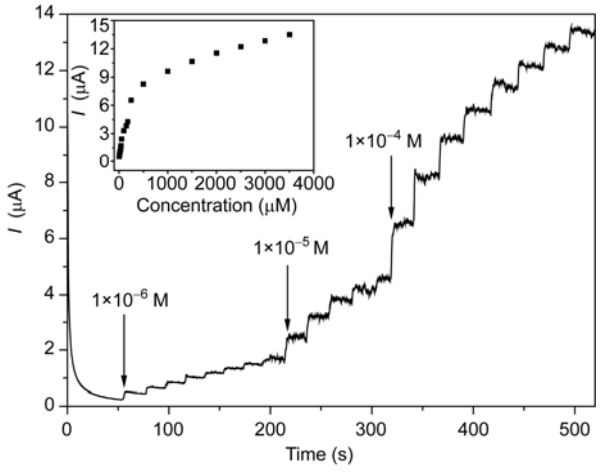

Figure 8 Amperometric response of the biosensor to successive addition of DA in 0.1 M pH 6.0 PBS at an applied potential of 375 mV. Insert shows calibration curve for the peak current and the concentration of DA.

4 Conclusions

In this work, N-CNTs/PANI nanocomposites were successfully fabricated by self-assembly method. The morphology, composition, and optical properties of the resulting products were characterized by TEM, TGA, FT-IR, UV-vis, and CV. The CV results showed that N-CNTs/PANI nanocomposites had excellent redox activity not only in acidic but also in neutral environment. A highly selective dopamine biosensor could be constructed based on the particular characteristic of N-CNTs/PANI nanocomposites. The biosensor could detect DA at its very low concentration in the presence of AA in an neutral environment. Furthermore, the biosensor showed good reproducibility and stability.

This work was supported by the National Natural Science Foundation of China (20905038, 20903057, 20974046, 50803027, 20874048 & 20804020), the National Basic Research Program of China (2009CB930600), the Natural Science Foundation of Jiangsu Province (08KJB150011 & 09KJB150007), and the Fok Ying-Tong Education Foundation under Grant 111051.

1 Chakraborty S, Raj CR. Amperometric biosensing of glutamate using carbon nanotube based electrode. *Electrochem Commun*, 2007, 9: 1323–1330
2 Gligor D, Varodi C, Muresan LM. Graphite electrode modified with a new phenothiazine derivative and with carbon nanotubes for NADH electrocatalytic oxidation. *Chem Biochem Eng Q*, 2010, 24: 159–166
3 Cui HF, Cui YH, Sun YL, Zhang K, Zhang WD. Enhancement of dopamine sensing by layer-by-layer assembly of PVI-dmeOs and nafion on carbon nanotubes. *Nanotechnology*, 2010, 21: 215601
4 Kumar SA, Chen SL, Chen SM. Electrochemical sensing of H_2O_2 at flavin adenine dinucleotide/chitosan/CNT nanocomposite modified electrode. *Electrochem Solid-State Lett,* 2010, 13: k83–k86
5 Cruz-Silva E, Cullen DA, Gu L, Romo-Herrera JM, Munoz-Sandoval E, Lopez-Urias F, Sumpter BG, Meunier V, Charlier JC, Smith DJ, Terrones H, Terrones M. Heterodoped nanotubes: Theory, synthesis, and characterization of phosphorus-nitrogen doped multiwalled car-

bon nanotubes. *ACS nano*, 2008, 2: 441–448
6 Lee SU, Belosludov RV, Mizuseki H, Kawazoe Y. Designing nanogadgetry for nanoelectronic devices with nitrogen-doped capped carbon nanotubes. *Small*, 2009, 5: 1769–1775
7 Xiong Y, Li Z, Guo Q, Xie Y. Synthesis of multi-walled and bamboo-like well-crystalline CN*x* nanotubes with controllable nitrogen concentration (x = 0.05–1.02). *Inorg Chem,* 2005, 44: 6506–6508
8 Tang YF, Allen BL, Kauffman DR, Star A. Electrocatalytic activity of nitrogen-doped carbon nanotube cups. *J Am Chem Soc*, 2009, 131: 13200–13201
9 Yang Y, Li X, Jiang J, Du H, Zhao L, Zhao Y. Control performance and biomembrane disturbance of carbon nanotube artificialWater channels by nitrogen-doping. *ACS nano*, 2010, 4: 5755–5762
10 Yano J, Kohno T, Kitani A. Electrochemical preparation of polyaniline microspheres incorporated with DNA. *J Appl Electrochem*, 2009, 39: 747–750
11 Jia P, Argun AA, Xu J, Xiong S, Ma J, Hammond PT, Lu X. Enhanced electrochromic switching in multilayer thin films of polyaniline-tethered silsesquioxane nanocage. *Chem Mater*, 2009, 21: 4434–4441
12 Gharibi H, Kakaei K, Zhiani M. Platinum nanoparticles supported by a vulcan XC-72 and PANI doped with trifluoromethane sulfonic acid substrate as a new electrocatalyst for direct methanol fuel cells. *J Phys Chem C*, 2010, 114: 5233–5240
13 Shao D, Hu J, Chen C, Sheng G, Ren X, Wang X. Polyaniline multiwalled carbon nanotube magnetic composite prepared byplasma-induced graft technique and its application for removal of aniline and phenol. *J Phys Chem C*, 2010, 114: 21524–21530
14 Tang Q, Wu J, Sun X, Li Q, Lin J. Shape and size control of oriented polyaniline microstructure by a self-assembly method. *Langmuir*, 2009, 25: 5253–5257
15 Mumtaz M, Labrugere C, Cloutet E, Cramail H. Synthesis of polyaniline nano-objects using poly(vinyl alcohol)-, poly(ethylene oxide)-, and poly[(*n*-vinyl pyrrolidone)-co-(vinyl alcohol)]-based reactive stabilizers. *Langmuir*, 2009, 25: 13569–13580
16 Li L, Qin ZY, Xia X, Fan QQ, Lu YQ, Wu WH, Zhu MF. Facile fabrication of uniform core shell structured carbon nanotube-polyaniline nanocomposites. *J Phys Chem C*, 2009, 113: 5502–5507
17 Guo L, Peng Z. One-pot synthesis of carbon nanotube-polyaniline-gold nanoparticle and carbon nanotube-gold nanoparticle composites by using aromatic amine chemistry. *Langmuir*, 2008, 24: 8971–8975
18 Komathi S, Gopalan AI, Lee KP. Covalently linked silica-multiwall carbon nanotube-polyaniline network: An electroactive matrix for ultrasensitive biosensor. *Biosens Bioelectron*, 2009, 25: 944–947
19 Yue B, Ma YW, Tao HS, Yu LS, Jian GQ, Wang XZ, Wang XS, Lu YN, Hu Z. CNx nanotubes as catalyst support to immobilize platinum nanoparticles for methanol oxidation. *J Mater Chem*, 2008, 18: 1747–1750
20 Bhadra S, Singha NK, Khastgir D. Electrochemical synthesis of polyaniline and its comparison with chemically synthesized polyaniline. *J Appl Polym Sci*, 2007, 104: 1900–1904
21 Bhadra S, Singha NK, Khastgir D. Mechanical, dynamic mechanical, morphological, thermal behavior and processability of polyaniline and ethylene 1-octene based semi-conducting composites. *J Appl Polym Sci*, 2008, 107: 2486–2493
22 Bhadra S, Singha NK, Chattopadhyay S, Khastgir D. Effect of different Reaction parameters on the conductivity and dielectric properties of polyaniline synthesized electrochemically and modeling of conductivity against reaction parameters through regression analysis. *J Polym Sci, Part B: Polym Phys*, 2007, 45: 2046–2059
23 Salvatierra RV, Oliveira MM, Zarbin AJG. One-pot synthesis and processing of transparent, conducting, and freestanding carbon nanotubes/polyaniline composite films. *Chem Mater*, 2010, 22: 5222–5234
24 Wei D, Ivaska A. Electrochemical biosensors based on polyaniline. *Chem Anal*, 2006, 51: 839–852
25 Xu L, Zhu Y, Yang X, Li C. Amperometric biosensor based on carbon nanotubes coated with polyaniline/dendrimer-encapsulated Pt nanoparticles for glucose detection. *Mater Sci Eng C*, 2009, 29: 1306–1310
26 Wu X, Zhao B, Wu P, Zhang H, Cai C. Effects of ionic liquids on enzymatic catalysis of the glucose oxidase toward the oxidation of glucose. *J Phys Chem B*, 2009, 113: 13365–13373
27 Chen D, Wang Q, Jin J, Wu P, Wang H, Yu S, Zhang H, Cai C. Low-potential detection of endogenous and physiological uric acid at uricase-thionine single-walled carbon nanotube modified electrodes. *Anal Chem*, 2010, 82: 2448–2455
28 Ding H, Long Y, Shen J, Wan M. $Fe_2(SO_4)_3$ as a binary oxidant and dopant to thin polyaniline nanowires with high conductivity. *J Phys Chem B*, 2010, 114: 115–119
29 Yan W, Feng X, Chen X, Li X, Zhu JJ. A selective dopamine biosensor based on AgCl@polyaniline core-shell nanocomposites. *Bioelectrochem*, 2008, 72: 21–27
30 Liu J, Tian S, Knoll W. Properties of polyaniline/carbon nanotube multilayer films in neutral solution and their application for stable low-potential detection of reduced β-nicotinamide adenine dinucleotide. *Langmuir*, 2005, 21: 5596–5599
31 Liu Y, Feng X, Shen J, Zhu JJ, Hou W. Fabrication of a novel glucose biosensor based on a highly electroactive polystyrene/polyaniline/Au nanocomposite. *J Phys Chem B*, 2008, 112: 9237–9242
32 Makos MA, Kim YC, Han KA, Heien ML, Ewing AG. *In vivo* electrochemical measurements of exogenously applied dopamine in drosophila melanogaster. *Anal Chem*, 2009, 81: 1848–1854
33 Kan X, Zhao Y, Geng Z, Wang Z, Zhu JJ. Composites of multiwalled carbon nanotubes and molecularly imprinted polymers for dopamine recognition. *J Phys Chem C*, 2008, 112: 4849–4854
34 Beni V, Ghita M, Arrigan DWM. Cyclic and pulse voltammetric study of dopamine at the interface between two immiscible electrolyte solutions. *Biosens Bioelectron*, 2005, 20: 2097–2103
35 Feng XM, Mao CJ, Yang G, Hou WH, Zhu JJ. Polyaniline/Au composite hollow spheres: synthesis, characterization, and application to the detection of dopamine. *Langmuir*, 2006, 22: 4384–4389